

# Simulation and process optimization of oil tank investment casting based on JSCAST

# Pan Yue<sup>1,3</sup>, \*Hua Hou<sup>1,3</sup>, and \*Yu-hong Zhao<sup>1,2,4</sup>

(1. School of Materials Science and Engineering, MOE jointly Collaborative Innovation Center for High-perforce Al/Mg based Materials, Shanxi Key Laboratory of Intelligent Casting and Advanced Forming for New Materials, North University of China, Taiyuan 030051, China; 2. Beijing Advanced Innovation Center for Materials Genome Engineering, University of Science and Technology Beijing, Beijing 100083, China; 3. School of Materials Science and Engineering, Taiyuan University of Science and Technology, Taiyuan 030024, China; 4. Institute of Materials Intelligent Technology, Liaoning Academy of Materials, Shenyang 110004, China)

\*Corrresponding address: e-mail: houhua@nuc.edu.cn, zhaoyuhong@nuc.edu.cn

**Abstract:** The filling process of oil tank castings with different pouring temperature, pouring speed and cavity temperature was simulated by JSCAST casting simulation software. The results show that changing the pouring temperature has no significant effect on the temperature field during the filling process. Higher cavity temperature can increase the temperature gradient of different parts of the casting, which is conducive to the formation of sequential solidification. In addition, the higher filling speed will lead to the peak velocity at the top and bottom of the casting, which is easy to cause air entrapment. In summary, the pouring speed of 3 kg/s, the mold temperature of 500 °C, and the pouring temperature of 720 °C are the best combination of process parameters for the tank casting.

Key Words: Investment casting, JSCAST, Oil tank, Numerical simulation

### 1 Introduction

Complex thin-walled aluminum alloy investment castings are increasingly widely used in aviation and aerospace due to their light weight, precise dimensions and high reliability [1-3]. The casting forming problem is one of the key technologies for studying this type of castings. Investment casting is a precision casting technique. It involves coating multiple layers of refractory materials on the surface of a wax mold, heating the wax mold to melt it and form a shell, and then pouring molten metal to obtain the casting [4, 5]. This technology can produce castings with high surface finish and high dimensional accuracy, and is suitable for the production of parts with complex shapes and high precision requirements. In the aviation field, investment casting is widely used in the manufacturing of key components such as engine mounts and turbine guides [6,7]. The traditional casting technology mainly relies on experience and experiments. The design process is mainly based on experience and the data from previous experiments. This design method shows obvious deficiencies for the production of large and medium-sized castings with complex structures. A large number of experiments will also greatly prolong the experiment cycle and the cost is difficult to control [8, 9]. In recent

years, with the development of casting numerical simulation technology, it has become possible to effectively predict defects before the actual production of castings [10]. Optimizing the casting process through simulation results is of great significance for improving the quality of castings and production efficiency and reducing production costs, which greatly promotes the upgrading of the traditional casting industry [11-13]. Pouring temperature and pouring speed are significant process parameters in the casting process. To obtain qualified castings, it is not only necessary to ensure the qualified composition of the molten iron, but also the pouring temperature of the molten iron is a key factor in the pouring process [14-17]. In this paper, the JSCAST casting simulation software was used to study the temperature field and velocity field during the filling process of the ZL114A oil tank casting under different pouring temperatures, cavity temperatures and pouring speeds, and the influence of these factors on the filling process was analyzed, which can provide a basis for the formulation of the oil tank casting process.

## 2 Experimental section

The casting material selected for the test is ZL114A, and its chemical composition is shown in Table 1 [18]. The

tensile strength in the as-cast state is  $\geq 310 \text{MPa}$ , and the elongation is  $\geq 3\%$  [19]. The shaping materials are divided into the surface layer and the back layer. The surface layer uses zircon sand, and the back layer uses mullite. The main material parameters used for casting temperature field simulation include density, specific heat capacity, thermal conductivity, etc. The thermophysical performance parameters of the test materials are shown in Tables 1, 2, 3 and 4 [20-22].

Table 1. Chemical Composition of ZL114A (wt. %)

Composition	Si	Mg	Ti	Al
Fraction	6.5~	0.45~	0.08~	Bal
	7.5	0.75	0.25	

Table 2. Thermophysical parameters of Casting materials

Туре	Value
Name	ZL114A
Density	$2.4080 \text{ g/cm}^3$
Specific heat	1.19 J/(g*°C)
Thermal conductivity	0.653 J/(cm*s*°C)
Solidification temperature	550.00 °C
Melting temperature	611.00 °C
Latent heat	$4.25*10^5 \text{ J/Kg}$
Dynamic viscosity	$0.005736 \text{ cm}^2\text{/s}$
Coefficient of linear expansion	1.700e-05 1/°C
Young's modulus	5.8840e+4 MPa/cm <sup>2</sup>
Poisson ratio	0.33

Table 3. Thermophysical parameters of the surface layer material of the mold shell

	-	
Surface	Value	
Name	Zircon sand	
Density	5.68~5.91 g/cm <sup>3</sup>	
Thermal expansion coefficient	7.5~13e-6 1/°C	
Thermal conductivity	14 W/(K*m)	
Dynamic viscosity coefficient	$0.01 \text{ cm}^2/\text{s}$	

Table 4. Thermophysical parameters of the back layer material of the mold shell

Back	Value
Name	Mullite
Density	$3.16 \text{ g/cm}^3$
Thermal expansion coefficient	4.2e-6 1/°C
Thermal conductivity	5 W/(K*m)

The contour dimensions of the fuel tank are 1198mm×650mm×564mm, and it is a large casting. According to the analysis of the structural features of the casting, due to the large overall size and thin wall thickness of the oil tank, there are very high requirements for the dimensional accuracy and quality of the casting at the same time. In the structure of the fuel tank, there are some ribs and bosses to fix the circuit system. These ribs, bosses and the tank wall form a large wall thickness jump, and hot cracking and shrinkage porosity are prone to occur at the junction of the thick and thin positions of the casting [23]. To reduce the weight, some deep grooves were added locally to the casting, and thin-walled heat dissipation fins were added to the box wall. Due to the above-mentioned characteristics of the fuel tank structure, it is comprehensively considered to adopt the investment casting process to improve the filling capacity of the molten metal and enhance the feeding effect of the molten metal on the castings, thereby obtaining high-quality castings. According to the characteristics of the difficulty in shell-making the grooves on the side wall of the fuel tank and the numerous large planar protrusions inside, the casting tree assembly scheme with simultaneous solidification is selected. Gap gates are set on the left and right sides and the lower surface of the casting for filling. The geometric model of the casting and the gating system is shown in Figure 1.

Based on the above design, a geometric model is established, and then the geometric model is meshed. To improve the simulation accuracy and operational efficiency at the same time, a minimum division interval of 5mm is adopted, the total number of model meshes is 8.19 million, and the number of casting meshes is 540,000. Assign the corresponding material performance parameters to the grid model units, set the thermal boundary conditions and initial conditions. The ambient temperature is 20° C. The heat transfer coefficient between and the molten metal the shell 0.01cal/(cm<sup>2</sup>·s·°C), and the heat transfer coefficient between the molten metal and the air is 0.0005cal/(cm²·s·°C). The heat transfer coefficient between the mold and air is 0.0005cal/(cm²·s·°C).

The pouring process parameters mainly include pouring temperature, pouring speed and cavity temperature. The following 8 groups of process parameters (as shown in Table 5 below) were simulated and studied by using the three-factor two-level

comprehensive test method.



Figure 1. Three-dimensional model of the casting and gating system

Table 5. Comprehensive test process parameters

Process	Pouring temperature °C	Shell temperature °C	Pouring speed kg/s	Cooling method
1	720	400	3	Room temperature
2	720	400	5	
3	720	500	3	
4	720	500	5	
5	730	400	3	
6	730	400	5	
7	730	500	3	
8	730	500	5	

#### 3 Results and discussion

# 3.1 Temperature field during filling process

The temperature distribution at the end of filling for the 8 groups of processes is shown in Figure 2 below. The color change from blue (at a temperature of 550 °C) to red (at a temperature of 720 °C) represents the temperature distribution of the molten metal. By comparing (a) and (e) (processes 1 and 5), (b) and (f) (processes 2 and 6), (c) and (g) (processes 3 and 7), (d) and (h) (processes 4 and 8), it can be known that the pouring temperature has little influence on the temperature field during the filling process. This is because the variation range of the pouring temperature is 10 °C, approximately 14%. Therefore, the influence is less than that of the cavity temperature and the pouring speed. By comparing (a) and (c) (processes 1 and 3), (b) and (d) (processes 2 and 4), (e) and (g) (processes 5 and 7), (f) and (h) (processes 6 and 8) among them, it can be known that when the cavity temperature is 500 °C, the temperature distribution of the casting conforms to sequential solidification, and when the cavity temperature is 400 °C, the temperature distribution is relatively uniform. Therefore, increasing the cavity temperature is conducive to forming sequential

solidification conditions. In conclusion, the process with a cavity temperature of 500 °C is superior, and the pouring temperature of 720 °C or 730 °C has no significant influence on the temperature field during the filling process.

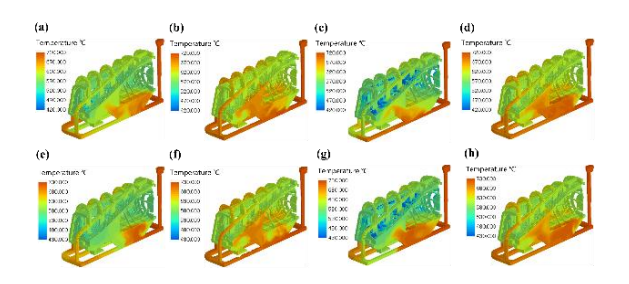


Figure 2. shows the temperature field of the three-factor two-level comprehensive test filling process, where (a) to (h) correspond to processes 1 to 8 respectively

The boundary conditions of the pouring speed of Process 3 being 3 kg/s, the mold temperature being 500 °C, and the pouring temperature being 720 °C respectively were selected to complete the numerical simulation of the oil tank filling process, as shown in Figure 3. It can be seen that the molten metal first enters the mold shell along the main runner, and then fills the

bottom cross runner under the action of gravity. When the pouring duration is 15 seconds, the bottom pouring tray in the pouring system is filled, and the side gates and the bottom of the casting begin to be filled. At this time, the temperature distribution of the alloy liquid everywhere is uniform. When the pouring duration is 18 seconds, the bottom of the casting is about to be filled completely, and the temperature distribution is uniform and higher than 670 °C. When the pouring duration is 28 seconds, the top and side walls of the fuel tank are filled by the side injection runner. Due to the relatively thin wall thickness of this part, its distance from the bottom runner, and the slow filling speed of the side injection runner, the temperature of the top and side walls drops to about 600 °C, and underfilling may occur. When the pouring duration is 34 seconds, the filling is completed. The temperature in the area at the top of the casting far from the direct runner and the gap runner drops to about 570 °C. The temperatures of both the bottom and side runner are above 600 °C, and the feeding can continue.

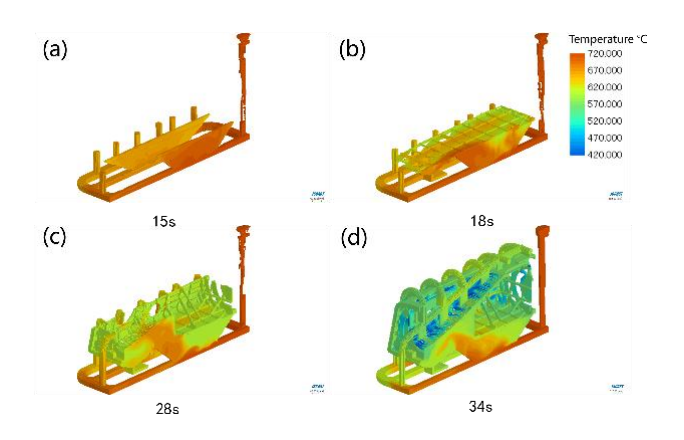


Figure 3. Temperature field of the filling process in Process 3

The temperature distribution at the end of the filling process in the 8 groups of processes is shown in Figure 4. The color change from blue (at a speed of 0 cm/s) to red (at a speed of 100 cm/s) represents the velocity distribution of the molten metal. By comparing (a) and (b) (processes 1 and 2), (c) and (d) (processes 3 and 4), (e) and (f) (processes 5 and 6), (g) and (h) (processes 7 and 8) among them, it can be known that the velocity distribution is more uniform when the pouring speed is 3 kg/s, and there are velocity peaks in the inner runner at the top and bottom of the casting when the pouring speed is 5 kg/s. Air entrapment may occur at the blind cavity. To

sum up, the process with a pouring speed of 3 kg/s is superior.

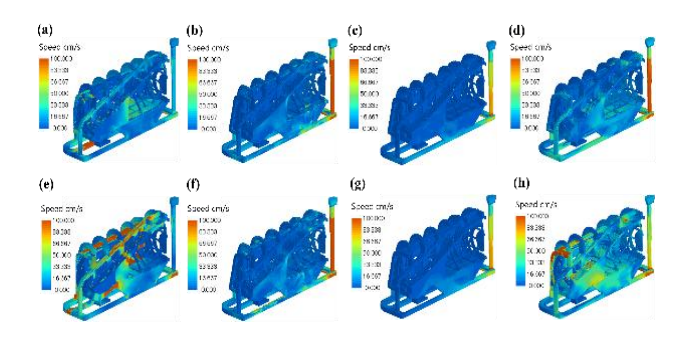


Figure 4. shows the velocity field during the filling process of the three-factor two-level comprehensive test

The boundary conditions of the pouring speed of Process 3 being 3 kg/s, the mold temperature being 500 °C, and the pouring temperature being 720 °C respectively were selected to complete the numerical simulation of the oil tank, as shown in Figure 5. It can be seen that the molten metal flows through the slit direct runner and the transverse runner into the cavity. When the pouring duration is 15 seconds, due to the hindering effect of the slit direct runner, the velocity of the molten metal at all points is lower than 0.38 m/s, which ensures the stability of the subsequent filling. From 18 seconds to 34 seconds, the molten metal is further decelerated through the bottom injection slot runner and the side injection runner, steadily filling the top and side walls of the casting until the filling is completed. Considering that the maximum speed in the direct runner can reach more than 100 cm/s, it indicates that the adoption of the double-gap direct runner significantly reduces the impact of the metal melt on the mold shell.

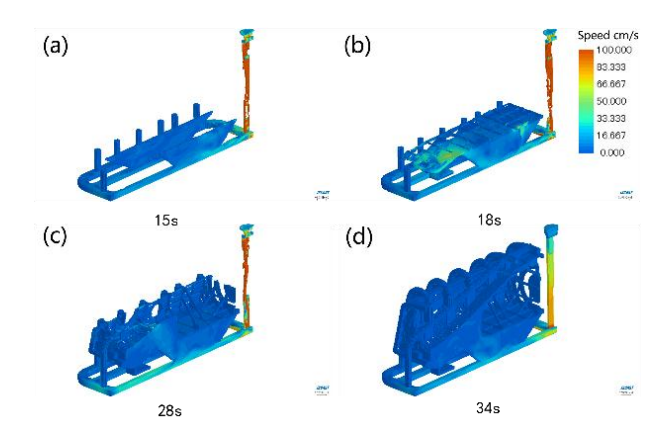


Figure 5. Velocity field of the filling process in Process 3

#### 4 Conclusion

- (1) The pouring temperature has no significant influence on the temperature distribution during the filling process. Increasing the cavity temperature can increase the temperature gradient at different parts of the pouring system, which is more in line with the sequential solidification conditions.
- (2) Increasing the pouring speed will lead to the problem of overly fast filling speed at the top and bottom of the casting, which may cause air entrapment in these areas.
- (3) The optimal combination of process parameters for this oil tank casting is a pouring speed of 3 kg/s, a mold temperature of 500 °C, and a pouring temperature of 720 °C respectively.

#### **Conflicts of interest**

The authors declare that they have no known competing financial interests or personal relationships that could have appeared to influence the work reported in this paper.

#### References

- [1] Chi Y, Murali N, Chen G-C, et al. Rapid investment casting of nano-treated aluminum alloy 2024. Int. J. Adv. Manuf. Technol. 135(1-2): 473-483, https://doi.org/10.1007/s00170-024-14529-0
- [2] Thanabumrungkul S, Jumpol W, Meemongkol N, et al. Investment casting of semi-solid 6063 aluminum alloy using the GISS process. Mater. Res. Express. 10(7): 76501, https://doi.org/10.1088/2053-1591/ace1d3
- [3] Xiao Z, Lv Z, Nie S, et al. Numerical simulation and optimization of investment casting for complex thin-walled castings. Int. J. Metalcast. 18(1): 159–179, https://doi.org/10.1007/s40962-023-00990-2
- [4] Jahangiri M, Jahangiri M. Is it critical to fill the mold from bottom and control the ingate-velocity during vacuum investment casting of nickel-based superalloys? Int. J. Metalcast. doi:10.1007/s40962-025-01570-2, https://doi.org/10.1007/s40962-025-01570-2
- [5] Sun B, Wang J, Kang M, et al. Investment casting technology and development trend of superalloy ultra

- limit components. Acta Metall. Sin. 58(4): 412–427, https://doi.org/10.11900/0412.1961.2021.00569
- [6] Chatterjee D, Chauhan A S, Venkat, et al. Realization of high pressure turbine blades of a small turbo-fan engine through investment casting process. Def. Sci. J. 73(2): 219–229, https://doi.org/10.14429/dsj.73. 18719
- [7] Hao X, Liu G, Wang Y, et al. Optimization of investment casting process for K477 superalloy aero-engine turbine nozzle by simulation and experiment. China Foundry. 19(4): 351–358, https://doi.org/10.1007/s41230-022-1092-4
- [8] Guo L, Mann W, Chen K, et al. Design and experimental validation of rapid hot isostatic pressing process for Ti6Al4V alloy. Int. J. Metalcast. . doi:10.1007/s40962-024-01522-2,https://doi.org/10.1 007/s40962-024-01522-2
- [9] Melali P, Boutorabi S M A, Divandari M. The effect of casting revert-virgin alloy with different portions on the microstructure and mechanical properties of 1.4930 heat-resistant stainless-steel alloy in investment casting process. Int. J. Metalcast. 18(3): 2119–2132,https://doi.org/10.1007/s40962-023-01144-0
- [10] Zhao D, Zhou L, Wang D, et al. Integrated computational framework for controlling dimensional accuracy of thin-walled turbine blades during investment casting. Int. J. Adv. Manuf. Technol. 129(3-4): 1315-1328, https://doi.org/ 10.1007/s00170-023-12319-8
- [11] Albuquerque C E S, Silva P C S, Grassi E N D, et al. Optimizing the gating system for rapid investment casting of shape memory alloys: computational numerical analysis for defect minimization in a simple-cubic cell structure. Metals. 13(6): 1138, https://doi.org/10.3390/met13061138
- [12] Liao Q, Ge P, Lu G, et al. Simulation study on the investment casting process of a low-cost titanium alloy gearbox based on ProCAST. Adv. Mater. Sci. Eng. 2022: 4484762, https://doi.org/10.1155/ 2022/4484762
- [13] Zhang P, Liu G, Wang Y, et al. Optimization of investment casting parameters for reduction of shrinkage porosity in nickel-based superalloy castings by taguchi method. Int. J. Modern Phys. B.

- 35(10): 2150136, https://doi.org/10.1142/ S0217979221501368
- [14] Wang S, Pan J, Chen R, et al. Orthogonal parameter optimization of K435 turbine blades manufactured by investment casting based on physical field analysis and microstructure prediction. Int. J. Heat Mass Transfer. 246: 127106, https://doi.org/10.1016/j.ijheatmasstransfer.2025.127106
- [15] Xie S, Lv Z, Dong S. Study on the optimization of investment casting process of exhaust elbow for high-power engine. Metals. 14(4): 481, https://doi.org/10.3390/met14040481
- [16] Zhao D, Wang D, Zhou L, et al. Effect of mold dwell time on shrinkage defects in investment casting of superalloy turbine blade. Int. J. Adv. Manuf. Technol. 132(9–10): 4473–4487, https://doi.org/10.1007/s00170-024-13659-9
- [17] 이종래. A study on structure of feed sprue considering turbulence and mold temperature in the investment casting process. 한국결정성장학회지. 32(1): 25-32, https://doi.org/10.6111/JKCGCT. 2022.32.1.025
- [18] Zhong C, Fang C, Wang R, et al. Research on two-stage solution treatment process of ZL114A alloy. Rare Met. Mater. Eng. 51(12): 4788–4792

- [19] Tao J, Xiang L, Chen X, et al. Study on Tensile Properties and Microstructures of Different Sites in Al-Si Alloy Casting Component. Arch. Metall. Mater. 68(2): 585–589, https://doi.org/10.24425/amm. 2023.142438
- [20] Zhang A, Liang S, Guo Z, et al. Determination of the interfacial heat transfer coefficient at the metal-sand mold interface in low pressure sand casting. Exp. Therm Fluid Sci. 88: 472–482, https://doi.org/10.1016/j.expthermflusci.2017.07.002
- [21] Bahtli T, Erdem Y. The use of foundry waste sand from investment casting in the production of porcelain tiles. Ceram. Int. 48(19): 27967–27972, https://doi.org/10.1016/j.ceramint.2022.06.100
- [22] Lu Y, Shi H, Lu K, et al. Properties and fracture mechanism of composite plaster mold covered with multiple adhesion layer for investment casting. Int. J. Metalcast. 18(2): 1770–1782, https://doi.org/10.1007/s40962-023-01152-0
- [23] Xiao Y, Xiao C, Chang D, et al. Time-varying disturbances of temperature field in investment casting and corresponding shrinkage defects control methods. J. Mater. Res. Technol. 35: 5147–5159, https://doi.org/10.1016/j.jmrt.2025.02.164